

Femtosecond Cr:LiSAF and Cr:LiCAF lasers pumped by tapered diode lasers

Umit Demirbas,^{1,4,*} Michael Schmalz,¹ Bernd Sumpf,² Götz Erbert,² Gale S. Petrich,³ Leslie A. Kolodziejski,³ James G. Fujimoto,³ Franz X. Kärtner,³ and Alfred Leitenstorfer¹

¹Department of Physics and Center for Applied Photonics, University of Konstanz, D-78464 Konstanz, Germany

²Ferdinand-Braun-Institut, Leibniz Institut für Höchstfrequenztechnik, D-12489 Berlin, Germany

³Department of Electrical Engineering and Computer Science and Research Laboratory of Electronics, Massachusetts Institute of Technology, Cambridge, Massachusetts 02139, USA

⁴Department of Electrical and Electronics Engineering, International Antalya University, 07190 Antalya, Turkey

*umit79@alum.mit.edu

Abstract: We report compact, low-cost and efficient Cr:Colquiriite lasers that are pumped by high brightness tapered laser diodes. The tapered laser diodes provided 1 to 1.2 W of output power around 675 nm, at an electrical-to-optical conversion efficiency of about 30%. Using a single tapered diode laser as the pump source, we have demonstrated output powers of 500 mW and 410 mW together with slope efficiencies of 47% and 41% from continuous wave (cw) Cr:LiSAF and Cr:LiCAF lasers, respectively. In cw mode-locked operation, sub-100-fs pulse trains with average power between 200 mW and 250 mW were obtained at repetition rates around 100 MHz. Upon pumping the Cr:Colquiriite lasers with two tapered laser diodes (one from each side of the crystal), we have observed scaling of cw powers to 850 mW in Cr:LiSAF and to 650 mW in Cr:LiCAF. From the double side pumped Cr:LiCAF laser, we have also obtained ~220 fs long pulses with 5.4 nJ of pulse energy at 77 MHz repetition rate. These are the highest energy levels reported from Cr:Colquiriite so far at these repetition rates. Our findings indicate that tapered diodes in the red spectral region are likely to become the standard pump source for Cr:Colquiriite lasers in the near future. Moreover, the simplified pumping scheme might facilitate efficient commercialization of Cr:Colquiriite systems, bearing the potential to significantly boost applications of cw and femtosecond lasers in this spectral region (750-1000 nm).

©2011 Optical Society of America

OCIS codes: (140.3460) Lasers; (140.4050) Mode-locked lasers; (140.3580) Lasers, solid-state; (140.3480) Lasers, diode pumped; (140.5680) Rare earth and transition metal solid-state lasers.

References and links

1. P. F. Moulton, "Spectroscopic and laser characteristics of Ti:Al₂O₃," J. Opt. Soc. Am. B **3**(1), 125–133 (1986).
2. R. Ell, U. Morgner, F. X. Kärtner, J. G. Fujimoto, E. P. Ippen, V. Scheuer, G. Angelow, T. Tschudi, M. J. Lederer, A. Boiko, and B. Luther-Davies, "Generation of 5-fs pulses and octave-spanning spectra directly from a Ti:sapphire laser," Opt. Lett. **26**(6), 373–375 (2001).
3. J. Klein and J. D. Kafka, "The Ti:Sapphire Laser: The flexible research tool," Nat. Photonics **4**(5), 289 (2010).
4. P. W. Roth, A. J. Maclean, D. Burns, and A. J. Kemp, "Directly diode-laser-pumped Ti:sapphire laser," Opt. Lett. **34**(21), 3334–3336 (2009).
5. J. Harrison, A. Finch, D. M. Rines, G. A. Rines, and P. F. Moulton, "Low-threshold, cw, all-solid-state Ti:Al₂O₃ laser," Opt. Lett. **16**(8), 581–583 (1991).
6. P. W. Roth, A. J. Maclean, D. Burns, and A. J. Kemp, "Direct diode-laser pumping of a mode-locked Ti:sapphire laser," Opt. Lett. **36**(2), 304–306 (2011).
7. B. Resan, E. Coadou, S. Petersen, A. Thomas, P. Walther, R. Viselga, J.-M. Heritier, J. Chilla, W. Tulloch, and A. Fry, "Ultrashort pulse Ti:sapphire oscillators pumped by optically pumped semiconductor (OPS) pump lasers" in *Proc. SPIE*, 2008), 687116–687118.
8. A. Müller, O. B. Jensen, A. Unterhuber, T. Le, A. Stingl, K.-H. Hasler, B. Sumpf, G. Erbert, P. E. Andersen, and P. M. Petersen, "Frequency-doubled DBR-tapered diode laser for direct pumping of Ti:sapphire lasers generating sub-20 fs pulses," Opt. Express **19**(13), 12156–12163 (2011).

9. S. A. Payne, L. L. Chase, L. K. Smith, W. L. Kway, and H. W. Newkirk, "Laser performance of $\text{LiSrAlF}_6:\text{Cr}^{3+}$," *J. Appl. Phys.* **66**(3), 1051–1056 (1989).
10. L. K. Smith, S. A. Payne, W. L. Kway, L. L. Chase, and B. H. T. Chai, "Investigation of the laser properties of $\text{Cr}^{3+}:\text{LiSrGaF}_6$," *IEEE J. Quantum Electron.* **28**(11), 2612–2618 (1992).
11. S. A. Payne, L. L. Chase, H. W. Newkirk, L. K. Smith, and W. F. Krupke, " $\text{LiCaAlF}_6:\text{Cr}^{3+}$ a promising new solid-state laser material," *IEEE J. Quantum Electron.* **24**(11), 2243–2252 (1988).
12. J. F. Pinto, L. Esterowitz, and G. H. Rosenblatt, "Frequency tripling of a Q-switched Cr:LiSAF laser to the UV region," *IEEE J. Sel. Top. Quantum Electron.* **1**(1), 58–61 (1995).
13. U. Demirbas, D. Li, J. R. Birge, A. Sennaroglu, G. S. Petrich, L. A. Kolodziejski, F. X. Kaertner, and J. G. Fujimoto, "Low-cost, single-mode diode-pumped Cr:Colquiriite lasers," *Opt. Express* **17**(16), 14374–14388 (2009).
14. I. T. Sorokina, E. Sorokin, E. Wintner, A. Cassanho, H. P. Jenssen, and R. Szipöcs, "14-fs pulse generation in Kerr-lens mode-locked prismless Cr:LiSGaF and Cr:LiSAF lasers: observation of pulse self-frequency shift," *Opt. Lett.* **22**(22), 1716–1718 (1997).
15. S. Uemura and K. Torizuka, "Generation of 10 fs pulses from a diode-pumped Kerr-lens mode-locked Cr:LiSAF laser," *Jpn. J. Appl. Phys.* **39**(Part 1, No. 6A), 3472–3473 (2000).
16. P. C. Wagenblast, U. Morgner, F. Grawert, T. R. Schibli, F. X. Kärtner, V. Scheuer, G. Angelow, and M. J. Lederer, "Generation of sub-10-fs pulses from a Kerr-lens modelocked $\text{Cr}^{3+}:\text{LiCAF}$ laser oscillator using third order dispersion compensating double chirped mirrors," *Opt. Lett.* **27**(19), 1726–1728 (2002).
17. P. Wagenblast, R. Ell, U. Morgner, F. Grawert, and F. X. Kärtner, "Diode-pumped 10-fs $\text{Cr}^{3+}:\text{LiCAF}$ laser," *Opt. Lett.* **28**(18), 1713–1715 (2003).
18. B. Agate, B. Stormont, A. J. Kemp, C. T. A. Brown, U. Keller, and W. Sibbett, "Simplified cavity designs for efficient and compact femtosecond Cr:LiSAF lasers," *Opt. Commun.* **205**(1-3), 207–213 (2002).
19. S. Tsuda, W. H. Knox, and S. T. Cundiff, "High efficiency diode pumping of a saturable Bragg reflector-mode-locked Cr:LiSAF femtosecond laser," *Appl. Phys. Lett.* **69**(11), 1538–1540 (1996).
20. J. M. Hopkins, G. J. Valentine, B. Agate, A. J. Kemp, U. Keller, and W. Sibbett, "Highly compact and efficient femtosecond Cr:LiSAF lasers," *IEEE J. Quantum Electron.* **38**(4), 360–368 (2002).
21. J. M. Hopkins, G. J. Valentine, W. Sibbett, J. A. der Au, F. Morier-Genoud, U. Keller, and A. Valster, "Efficient, low-noise, SESAM-based femtosecond $\text{Cr}^{3+}:\text{LiSrAlF}_6$ laser," *Opt. Commun.* **154**(1-3), 54–58 (1998).
22. U. Demirbas, A. Sennaroglu, F. X. Kärtner, and J. G. Fujimoto, "Highly efficient, low-cost femtosecond $\text{Cr}^{3+}:\text{LiCAF}$ laser pumped by single-mode diodes," *Opt. Lett.* **33**(6), 590–592 (2008).
23. E. Sorokin, "Solid-state materials for few-cycle pulse generation and amplification," in *Few-cycle laser pulse generation and its applications*, F. X. Kärtner, ed. (Springer-Verlag, 2004), pp. 3–71.
24. F. Druon, F. Balebois, and P. Georges, "New laser crystals for the generation of ultrashort pulses," *C. R. Phys.* **8**(2), 153–164 (2007).
25. S. Tsuda, W. H. Knox, S. T. Cundiff, W. Y. Jan, and J. E. Cunningham, "Mode-locking ultrafast solid-state lasers with saturable Bragg reflectors," *IEEE J. Sel. Top. Quantum Electron.* **2**(3), 454–464 (1996).
26. U. Keller, K. J. Weingarten, F. X. Kärtner, D. Kopf, B. Braun, I. D. Jung, R. Fluck, C. Hönninger, N. Matuschek, and J. Aus der Au, "Semiconductor saturable absorber mirrors (SESAM's) for femtosecond to nanosecond pulse generation in solid-state lasers," *IEEE J. Sel. Top. Quantum Electron.* **2**(3), 435–453 (1996).
27. D. Kopf, K. J. Weingarten, G. Zhang, M. Moser, M. A. Emanuel, R. J. Beach, J. A. Skidmore, and U. Keller, "High-average-power diode-pumped femtosecond Cr:LiSAF lasers," *Appl. Phys. B* **65**(2), 235–243 (1997).
28. P. M. W. French, R. Mellish, J. R. Taylor, P. J. Delfyett, and L. T. Florez, "Mode-locked all-solid-state diode-pumped Cr:LiSAF laser," *Opt. Lett.* **18**(22), 1934–1936 (1993).
29. A. Isemann and C. Fallnich, "High-power Colquiriite lasers with high slope efficiencies pumped by broad-area laser diodes," *Opt. Express* **11**(3), 259–264 (2003).
30. U. Demirbas, A. Sennaroglu, A. Benedick, A. Siddiqui, F. X. Kärtner, and J. G. Fujimoto, "Diode-pumped, high-average power femtosecond $\text{Cr}^{3+}:\text{LiCAF}$ laser," *Opt. Lett.* **32**(22), 3309–3311 (2007).
31. U. Demirbas, A. Sennaroglu, F. X. Kärtner, and J. G. Fujimoto, "Comparative investigation of diode pumping for continuous-wave and mode-locked $\text{Cr}^{3+}:\text{LiCAF}$ lasers," *J. Opt. Soc. Am. B* **26**(1), 64–79 (2009).
32. R. Scheps, J. F. Myers, H. B. Serreze, A. Rosenberg, R. C. Morris, and M. Long, "Diode-pumped Cr:LiSrAlF₆ laser," *Opt. Lett.* **16**(11), 820–822 (1991).
33. G. J. Valentine, J. M. Hopkins, P. Loza-Alvarez, G. T. Kennedy, W. Sibbett, D. Burns, and A. Valster, "Ultralow-pump-threshold, femtosecond $\text{Cr}^{3+}:\text{LiSrAlF}_6$ laser pumped by a single narrow-stripe AlGaInP laser diode," *Opt. Lett.* **22**(21), 1639–1641 (1997).
34. U. Demirbas, G. S. Petrich, D. Li, A. Sennaroglu, L. A. Kolodziejski, F. X. Kärtner, and J. G. Fujimoto, "Femtosecond tuning of Cr:Colquiriite lasers with AlGaAs-based saturable Bragg reflectors," *J. Opt. Soc. Am. B* **28**(5), 986–993 (2011).
35. D. Li, U. Demirbas, J. R. Birge, G. S. Petrich, L. A. Kolodziejski, A. Sennaroglu, F. X. Kärtner, and J. G. Fujimoto, "Diode-pumped passively mode-locked GHz femtosecond Cr:LiSAF laser with kW peak power," *Opt. Lett.* **35**(9), 1446–1448 (2010).
36. B. Sumpf, K. H. Hasler, P. Adamiec, F. Bugge, F. Dittmar, J. Fricke, H. Wenzel, M. Zorn, G. Erbert, and G. Trankle, "High-brightness quantum well tapered lasers," *IEEE J. Sel. Top. Quantum Electron.* **15**(3), 1009–1020 (2009).
37. B. Sumpf, P. Adamiec, M. Zorn, H. Wenzel, and G. Erbert, "Nearly diffraction limited tapered lasers at 675 nm with 1 W output power and conversion efficiencies above 30%," *Photon. Technol. Lett.* **23**(4), 266–268 (2011).
38. P. Klopp, V. Petrov, U. Griebner, and G. Erbert, "Passively mode-locked Yb:KYW laser pumped by a tapered diode laser," *Opt. Express* **10**(2), 108–113 (2002).

39. H. P. H. Cheng, O. B. Jensen, P. Tidemand-Lichtenberg, P. E. Andersen, P. M. Petersen, B. Sumpf, G. Erbert, and C. Pedersen, "Efficient quasi-three-level Nd:YAG laser at 946 nm pumped by a tunable external cavity tapered diode laser," *Opt. Commun.* **283**(23), 4717–4721 (2010).
40. A. Robertson, R. Knappe, and R. Wallenstein, "Diode-pumped broadly tunable (809-910 nm) femtosecond Cr:LiSAF laser," *Opt. Commun.* **147**(4-6), 294–298 (1998).
41. S. Sakadžić, U. Demirbas, T. R. Mempel, A. Moore, S. Ruvinskaya, D. A. Boas, A. Sennaroglu, F. X. Kärtner, and J. G. Fujimoto, "Multi-photon microscopy with a low-cost and highly efficient Cr:LiCAF laser," *Opt. Express* **16**(25), 20848–20863 (2008).
42. K. A. Tillman, D. T. Reid, D. Artigas, J. Hellstrom, V. Pasiskevicius, and F. Laurell, "Low-threshold, high-repetition-frequency femtosecond optical parametric oscillator based on chirped-pulse frequency conversion," *J. Opt. Soc. Am. B* **20**(6), 1309–1316 (2003).
43. F. X. Kärtner, J. A. der Au, and U. Keller, "Mode-locking with slow and fast saturable absorbers - what's the difference?" *IEEE J. Sel. Top. Quantum Electron.* **4**(2), 159–168 (1998).
44. D. Findlay and R. A. Clay, "The measurement of internal losses in 4-level lasers," *Phys. Lett.* **20**(3), 277–278 (1966).
45. G. Lacayo, I. Hahnert, D. Klimm, P. Reiche, and W. Neumann, "Transmission electron microscope study of secondary phases in Cr³⁺:LiCaAlF₆ single crystals," *Cryst. Res. Technol.* **34**(9), 1221–1227 (1999).
46. D. Klimm and P. Reiche, "Ternary colquiriite type fluorides as laser hosts," *Cryst. Res. Technol.* **34**(2), 145–152 (1999).
47. D. Klimm and P. Reiche, "Nonstoichiometry of the new laser host LiCaAlF₆," *Cryst. Res. Technol.* **33**(3), 409–416 (1998).
48. D. Klimm, G. Lacayo, and P. Reiche, "Growth of Cr:LiCaAlF₆ and Cr:LiSrAlF₆ by the Czochralski method," *J. Cryst. Growth* **210**(4), 683–693 (2000).
49. M. Stalder, M. Bass, and B. H. T. Chai, "Thermal quenching of fluorescence in chromium-doped fluoride laser crystals," *J. Opt. Soc. Am. B* **9**(12), 2271–2273 (1992).
50. F. Balembois, F. Falcoz, F. Kerboull, F. Druon, P. Georges, and A. Brun, "Theoretical and experimental investigations of small-signal gain for a diode-pumped Q-Switched Cr:LiSAF laser," *IEEE J. Quantum Electron.* **33**(2), 269–278 (1997).
51. J. M. Eichenholz and M. Richardson, "Measurement of thermal lensing in Cr³⁺-doped colquiriites," *IEEE J. Quantum Electron.* **34**(5), 910–919 (1998).
52. U. Demirbas, K. H. Hong, J. G. Fujimoto, A. Sennaroglu, and F. X. Kärtner, "Low-cost cavity-dumped femtosecond Cr:LiSAF laser producing >100 nJ pulses," *Opt. Lett.* **35**(4), 607–609 (2010).
53. U. Demirbas, A. Benedick, A. Sennaroglu, D. Li, J. Kim, J. G. Fujimoto, and F. X. Kärtner, "Attosecond resolution timing jitter characterization of diode pumped femtosecond Cr:LiSAF lasers," in *CLEO*, (San Jose, California, 2010).
54. O. Gayer, Z. Sacks, E. Galun, and A. Arie, "Temperature and wavelength dependent refractive index equations for MgO-doped congruent and stoichiometric LiNbO₃," *Appl. Phys. B* **91**(2), 343–348 (2008).
55. U. Demirbas, A. Sennaroglu, F. X. Kärtner, and J. G. Fujimoto, "Generation of 15 nJ pulses from a highly efficient, low-cost multipass-cavity Cr³⁺:LiCAF laser," *Opt. Lett.* **34**(4), 497–499 (2009).
56. S. N. Tandon, J. T. Gopinath, H. M. Shen, G. S. Petrich, L. A. Kolodziejski, F. X. Kärtner, and E. P. Ippen, "Large-area broadband saturable Bragg reflectors by use of oxidized AlAs," *Opt. Lett.* **29**(21), 2551–2553 (2004).
57. L.-J. Chen, M. Y. Sander, and F. X. Kärtner, "Kerr-lens mode locking with minimum nonlinearity using gain-matched output couplers," *Opt. Lett.* **35**(17), 2916–2918 (2010).
58. K. Minoshima, A. M. Kowalevicz, I. Hartl, E. P. Ippen, and J. G. Fujimoto, "Photonic device fabrication in glass by use of nonlinear materials processing with a femtosecond laser oscillator," *Opt. Lett.* **26**(19), 1516–1518 (2001).
59. P. Theer, M. T. Hasan, and W. Denk, "Two-photon imaging to a depth of 1000 μm in living brains by use of a Ti:Al₂O₃ regenerative amplifier," *Opt. Lett.* **28**(12), 1022–1024 (2003).
60. F. Helmchen and W. Denk, "Deep tissue two-photon microscopy," *Nat. Methods* **2**(12), 932–940 (2005).

1. Introduction

The Ti:Sapphire gain medium (i) has an ultra-broad gain bandwidth supporting pulses as short as 5 fs as well as tunability from 680 to 1080 nm, and (ii) exhibits favorable thermal properties which enable power scaling to several watts [1,2]. Hence, Ti:Sapphire lasers successfully replaced dye laser technology in the early 1990s. Since then, they have played a crucial role in the laser market, especially for applications that benefit from flexibility in wavelength, pulse duration, and average power [3]. On the other hand, Ti:Sapphire crystals have rather high passive losses [4], which necessitates the usage of a relatively high output coupling (~10%) for efficient laser operation. Combined with the relatively low product of fluorescence lifetime and emission cross section ($130 \mu\text{s} \times 10^{-20} \text{cm}^2$), these high parasitic losses and the necessity to use high output coupling result in quite high lasing thresholds in Ti:Sapphire lasers [4,5]. Hence, one needs pump powers of 3-5 watts to reach reasonable output power levels (~500 mW) from Ti:Sapphire lasers. This requires the usage of high-

power frequency-doubled neodymium lasers as pump sources, which are relatively expensive and electrically inefficient. All of these factors limit the widespread adoption of Ti:Sapphire technology. Direct diode pumping of Ti:Sapphire gain medium with blue GaN diode lasers around 450 nm has been demonstrated recently [4,6]. However, upon pumping with a single 1-W diode ($M^2 \sim 1.5$), only 13 mW of average power and a pulse width of 114 fs have been obtained in cw mode-locked operation [6]. This result is partly due the disadvantages of Ti:Sapphire mentioned above, and partly due the existence of additional parasitic losses when exciting at such short wavelengths [6]. We also note that green sources based on frequency doubled semiconductor lasers are slowly becoming the standard pump for Ti:Sapphire [7]. Frequency doubled tapered diode lasers have also been recently demonstrated as a possible pump source for Ti:Sapphire [8]. Although these emerging technologies have benefits over standard Nd-based technology, the cost, complexity, and compactness are still a factor compared to direct diode pumping.

As the most promising alternative to Ti:Sapphire, Cr³⁺-doped colquiriite crystals (Cr³⁺:LiSAF [9], Cr³⁺:LiSGaF [10], and Cr³⁺:LiCAF [11]) also possess broad gain bandwidths around 800 nm, providing total tunability from 720 nm to 1065 nm [11–13] and enabling generation of pulses on a 10-fs level [14–17]. Furthermore, Cr³⁺:Colquiriite crystals can have very low passive losses. Since the product of their fluorescence lifetime and emission cross sections are also high ($320 \mu\text{s} \times 10^{-20} \text{ cm}^2$ for Cr:LiSAF), the lasing threshold in Cr:Colquiriites lasers can be quite low (~ 10 mW). Another advantage of Cr:Colquiriites are their high intrinsic slope efficiencies ($>50\%$), enabling efficient laser operation. More relevant here however is that, they have broad and relatively strong absorption bands around 650 nm, which allow for direct pumping by low-cost red laser diodes, significantly reducing system complexity and improving wall-plug efficiency [18–22]. On the other hand, compared to Ti:Sapphire, Cr:Colquiriites have low emission cross sections ($1.3 \times 10^{-20} \text{ cm}^2$ for Cr:LiCAF, 3% of Ti:Sapphire) and low third-order nonlinearity ($0.4 \times 10^{-16} \text{ cm}^2/\text{W}$ for Cr:LiCAF, 12% of Ti:Sapphire) [23,24]. Combined with the existence of Auger upconversion process, which limit the inversion densities one can get, the lower emission cross section results in lower gain, requiring the use of low-loss optics (especially for Cr:LiCAF). The lower emission cross section also increases the tendency of Cr:Colquiriites towards q-switching, which can be handled by smart design of the cavity elements. The low third-order nonlinearity makes Kerr-lens mode-locking (KLM) difficult, especially for designing a turn-key commercial system. However, saturable Bragg reflectors (SBRs) [25] (also referred as saturable absorber mirrors (SESAMs) [26]), can overcome this limitation to obtain stable, turn-key mode-locked operation.

Various diode types have been used to pump Cr:Colquiriite lasers to date, including laser diode arrays [27], broad-stripe single-emitter diodes [17,28–31], and single transverse-mode laser diodes (ridge waveguide lasers) [13,18–22,32–34]. One main drawback of these sources has been their relatively low brightness, requiring four to six diodes to reach reasonable output power levels [13,29,34,35]. For example, state-of-the-art single mode diodes at 650 nm provide about 170 mW of output power at $M^2 < 1.1$. This corresponds to a brightness (B) of about $360 \text{ mW}/\mu\text{m}^2$. Four of these diodes are needed to reach a cw output around 335 mW and average powers of about 250 mW in mode-locked operation [34]. Single-emitter diodes with 150 μm stripe width are commercially available and provide up to 1.5 W, but beam profiles are asymmetric and of low quality ($M_{\text{slow}}^2 \sim 10$, $M_{\text{fast}}^2 < 1.1$). Hence, even though they provide quite high output powers, their brightness ($\sim 340 \text{ mW}/\mu\text{m}^2$) is even lower than the single mode diodes. Therefore, one needs to combine two to four of these diodes to reach cw output levels of 590 mW and cw mode-locked average powers of 390 mW [31]. Moreover, the low quality pump beam limits the obtainable slope efficiencies to 19% in TEM00 laser operation, and also causes strong thermal load via Auger upconversion process due the unmatched pump volume [31]. Likewise, multimode diode arrays might exhibit very high power levels (10s of Watts), but at the expense of increased cost and reduced beam quality [27]. For example, Kopf et al. used a 15 W diode array ($M_{\text{slow}}^2 \sim 1200$, $M_{\text{fast}}^2 < 1.1$, $B \sim 28 \text{ mW}/\mu\text{m}^2$) to pump a specially designed Cr:LiSAF laser with an asymmetric cavity beam profile. Average powers of 1.42 W

and 500 mW were obtained in cw and cw mode-locked operation, respectively [27]. The low quality beam profile limited the cw slope efficiencies to 18% [27]. In summary, all studies performed so far have used complex pumping geometries to reach reasonable output levels from Cr:Colquiriite lasers due to the low brightness of the pump sources. Moreover, multimode diode pump sources with low beam quality induce strong thermal effects and only provide limited slope efficiencies in Cr:Colquiriite lasers [27,31]. Multimode diode pumped Cr:Colquiriite lasers sometimes also require special optics for improving mode-matching between the pump and cavity mode (like cylindrical cavity mirrors [27] and coated flat-Brewster cut crystals [29], etc.), which increases cost and complexity of the overall system.

As an alternative technology, tapered diodes combine the excellent beam quality of ridge waveguide lasers and the output power of broad-stripe single emitters [36,37]. Tapered diode lasers consist of a straight ridge waveguide section and a tapered section. Any higher-order modes generated in the tapered section are filtered out by the ridge waveguide, resulting in an almost diffraction-limited beam profile [36]. For example, tapered diodes at 980 nm have been successfully used for pumping solid-state lasers based on Ytterbium and Neodymium [38,39]. Note that there also exist devices based on the master oscillator power amplifier (MOPA) concept. In contrast to MOPA systems with several independent components operated in series, the entire chip acts as a resonator in the tapered diode [36]. In 1998, Robertson et al. used two hybrid MOPA devices providing 450 mW of output power each ($M^2 < 2$, $B \sim 260 \text{ mW}/\mu\text{m}^2$) to pump a Cr:LiSAF laser. They obtained femtosecond pulse trains with approximately 100 mW of average power and a tuning range from 809 nm to 910 nm [40].

In this work, we report the first successful application of monolithic high brightness tapered diode lasers (TDLs) to pump Cr:Colquiriite systems. A single device on a C-mount package [37] was used in the first set of experiments. It provided up to 1.2 W of output power at 675 nm together with M^2 ($1/e^2$) values of 1.1 in the fast axis and 2.6 in the slow axis, respectively. This corresponds to a brightness of about $1000 \text{ mW}/\mu\text{m}^2$, which is almost 3 times improvement in brightness compared to the state of the art single mode laser diodes ($360 \text{ mW}/\mu\text{m}^2$) and broad-stripe single-emitter diodes ($340 \text{ mW}/\mu\text{m}^2$). In the laser experiments with a single TDL pumped Cr:Colquiriites, we have obtained up to 500 mW and 410 mW of output power and slope efficiencies of 47% and 41% from Cr:LiSAF and Cr:LiCAF lasers in cw operation at 1150 mW of absorbed pump power. In typical mode locking experiments, 105-fs, 1.84-nJ pulses with 232 mW of average power around 800 nm, and 90-fs, 1.97-nJ pulses with 193-mW of average power around 850 nm have been obtained from the Cr:LiSAF laser. Similarly, in mode-locking experiments with Cr:LiCAF, 55-fs, 2.04-nJ pulses with 217 mW of average power around 800 nm have been achieved. To investigate power scalability, we have also built Cr:Colquiriite lasers pumped by two tapered diodes (one from each side). In this configuration, up to 850 mW and 650 mW of output power and slope efficiencies of 49% and 42% were demonstrated from Cr:LiSAF and Cr:LiCAF lasers in cw operation at 1750 mW of absorbed pump power, respectively. Using this high power system for mode-locking of Cr:LiCAF, we have also obtained ~ 220 fs long pulses centered around 810 nm, with 415 mW of average power. This corresponds to a pulse energy of 5.4 nJ at the repetition rate of 77 MHz. These are the highest energies obtained from standard Cr:Colquiriite oscillators to date. Overall, these results show that Cr:Colquiriite lasers pumped with tapered diodes could become attractive alternatives to Ti:Sapphire for various applications in science and technology such as multiphoton microscopy [41], OPO pumping [42], amplifier seeding, etc.

The paper is organized as follows: section 2 introduces the properties of the tapered diode lasers that were used in the experiments. Section 3 presents cw and cw mode-locked laser results that were obtained with the Cr:Colquiriite laser that was pumped by a single tapered diode laser. Section 4 discuss power scaling and presents cw and mode-locking results of the Cr:Colquiriite lasers that is pumped by two tapered diodes. Finally, in section 5, we summarize the results and provide a general discussion.

2. Specifications of the Tapered Diode Lasers (TDLs)

In this section, we will briefly describe the high-brightness tapered diode lasers (TDL) that were used to pump the Cr:Colquiriite lasers in this study. The TDLs were grown and characterized at the facilities of Ferdinand Braun Institute and detailed information on this class of diodes can be found in [37]. The first TDL (TDL-1, which was used in single TDL pumped Cr:Colquiriite experiments in Section 3) had a total cavity length of 2 mm, and consisted of a 500 μm long ridge waveguide section and a 1.5 mm long tapered amplifier section with a flared angle of 3° . The output aperture was 85 μm wide. The front facet of the TDL had a reflectivity of 1%, whereas the rear facet had a reflectivity of 94%. The device was mounted p-side down on copper tungsten submounts using AuSn solder, which was then mounted on standard C-mounts. A commercial temperature controlled c-mount diode fixture (ILX LDM-4409) was used in housing the diode. Figure 1 (left) shows the measured variation of optical output power with diode drive current at the diode holder temperatures of 15, 20 and 25 $^\circ\text{C}$. At 15 $^\circ\text{C}$, the diode had a lasing threshold of about 340 mA and a slope efficiency of about 1.1 W/A. The diode spectrum (Fig. 1 right) had a width of 1 nm and was centered around 676.5 nm at 15 $^\circ\text{C}$. At a drive current of 1.5 A, the diode provided up to 1180 mW of output power, with a diode voltage of 2.6 V, which corresponds to an electrical-to-optical conversion efficiency of about 30%. We note here that direct diode pumping with such an efficient diode provides a significant advantage to Cr:Colquiriites over Ti:Sapphire in terms of the overall electrical-to-optical conversion efficiency of the system.

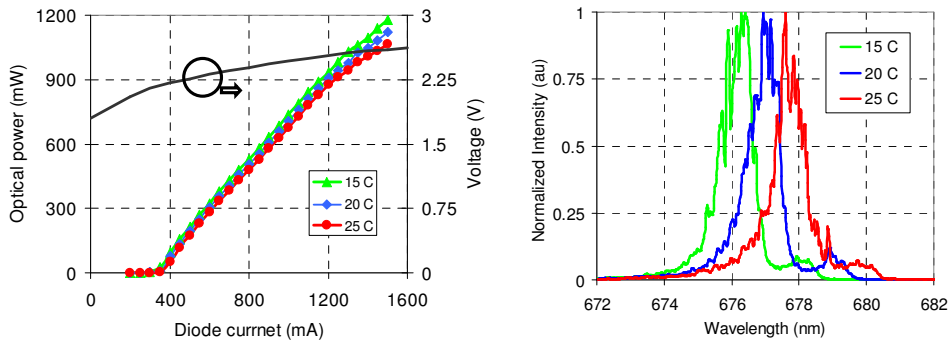


Fig. 1. (Left) Measured variation of optical output power with input current for the first tapered diode laser (TDL-1) at the diode holder temperatures of 15, 20 and 25 $^\circ\text{C}$. Corresponding voltage values of TDL-1, for 25 $^\circ\text{C}$ operation were also shown. (Right) Measured optical spectrum of the diode at 1.4 A diode current, and at the diode holder temperatures of 15, 20 and 25 $^\circ\text{C}$.

The beam quality of the TDLs has been measured by applying the method of the moving slit (ISO Standard 11146, Annex A). The intensity profiles of the beam waist and the far field, as well as the near-field, i.e. the intensity distribution along the front facet were measured. Also the astigmatism, i.e. the difference of the focal points in vertical and longitudinal direction were determined. For the measurements the laser spot was magnified by using a telescope with a magnification of about 60. Figure 2 shows the measured beam waist, far field and near field profiles of the first tapered diode laser in the slow axis. The measurements in Fig. 2 were carried out at an output power of 1 W, and at the diode holder temperature of 15 $^\circ\text{C}$. The measured beam waist is 28 μm at the $1/e^2$ -level. 80% of the emitted power originates from the central lobe of the beam waist. The corresponding far field angle is 4.5° ($1/e^2$), which leads to a beam propagation ratio of 2.6 ($1/e^2$). In the fast axis, we have measured a beam propagation ratio better than 1.1 at the $1/e^2$ level, and 1.5 using the second moments. Typical beam divergence in the fast axis was about 30° . The astigmatism of the diode (the difference between the positions of the vertical and lateral beam waist) is measured to be 700 μm . Based

on the above presented values, the brightness of the laser device was determined to be $B = 1000 \text{ mW}/\mu\text{m}^2$.

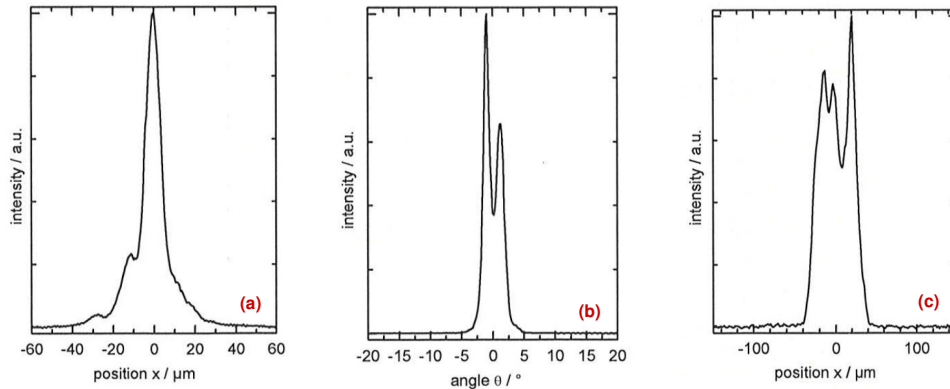


Fig. 2. (a) Beam waist, (b) far field and (c) near field profile for the slow axis of the first tapered diode laser (TDL-1) measured at 1 W of output power and at a cooling temperature of 15 °C.

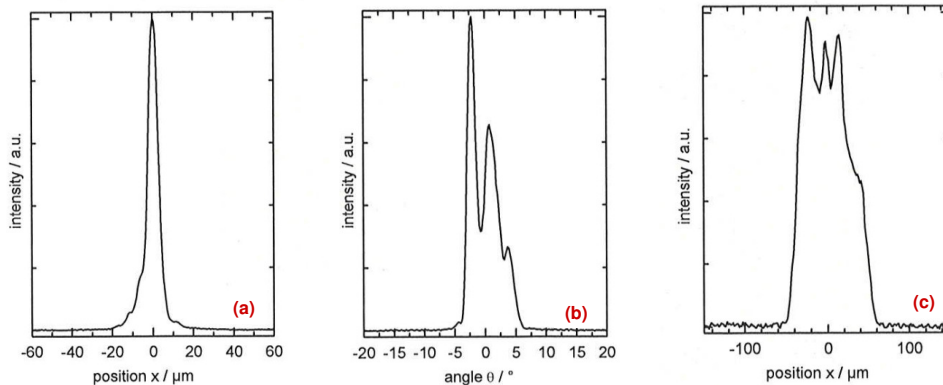


Fig. 3. (a) Beam waist, (b) far field and (c) near field profile for the slow axis of the second tapered diode laser (TDL-2) measured at 1 W of output power and at a cooling temperature of 15 °C.

The second tapered diode laser (TDL-2) that was used in double-side pumping experiments in Section 4, was very similar to TDL-1, which was described in detail above. The main difference was, TDL-2 had a flared angle of 4°, resulting in an output aperture size of 110 μm. TDL-2 also had a slightly higher lasing threshold (450 mA), and slightly lower slope efficiency (0.96 W/A), and provided 1035 mW of optical output power at a drive current of 1.5 A. 94% of the emitted power originates from the central lobe of the beam waist for TDL-2 (Fig. 3). The diode spectrum had a width of 0.8 nm and was centered around 678 nm at 15 °C. For TDL-2, we have measured the beam quality factor as 2.2 in the slow axis and as 1.1 in the fast axis (both at $1/e^2$ level).

3. Cr:Colquiriite Lasers Pumped by a Single Tapered Diode Laser

3.1 Experimental layout of the single TDL pumped Cr:Colquiriite laser

Figure 4 shows the setups of the Cr:LiSAF and Cr:LiCAF lasers that were pumped by a single tapered diode laser. The output of the tapered diode laser was first collected by an aspheric lens of a focal length of $f = 4.5 \text{ mm}$ and a numerical aperture of 0.54 ($f1$ in Fig. 4). This first lens also collimated the diode output in the slow axis. On the other hand, in the fast axis the

collecting lens actually focused the diode output, which is then collimated with a second cylindrical lens of a focal length of 50 mm (f_2). After passing through these two lenses, the beam shape becomes almost circular. An achromatic doublet with $f = 60$ mm was used to focus the pump beam into the crystal (f_2). Astigmatically-compensated, X-cavities with two curved pump mirrors (M1 and M2, $R = 75$ mm), a flat end mirror (HR), and a flat output coupler (OC) were employed in the cw laser experiments. The length of the long cavity arm was adjusted to obtain a beam waist of approximately $25 \mu\text{m}$ inside the gain medium, where as the short arm length was about 30 cm long in all the experiments. A 7-mm-long, 1.5% Cr-doped Cr:LiSAF and a 4-mm-long, 7% Cr-doped Cr:LiCAF crystal from VLOC were used in the studies. They absorbed 99.5% and 98.5% of the incident TM polarized pump light at 675 nm, respectively. Both crystals were 1.5 mm thick and mounted with indium foil in a copper holder under water cooling. Once lasing was obtained, the position of the 4.5 mm long collimating lens (f_1) and the 50 mm cylindrical lens (f_2) were fine adjusted to optimize the output power. This minimized the astigmatism of the pump beam at the focus, and hence optimized the mode matching between the laser and pump modes.

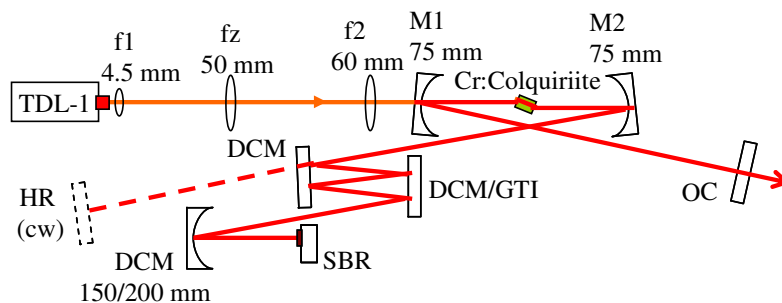


Fig. 4. Schematics of cw and cw mode-locked Cr:LiCAF/LiSAF oscillators pumped by a single tapered diode laser (TDL-1). Double chirped mirrors (DCMs) and/or Gires–Tournois interferometer (GTI) mirrors are used for dispersion compensation. SBR: Saturable Bragg reflector. M1-M2: Curved pump mirrors with a ROC of 75 mm. OC: Output coupler. f_1 : Collecting & collimating aspheric lens. f_z : Cylindrical collimating lens. f_2 : Focusing lens.

AlGaAs-based saturable Bragg reflectors (SBRs) were used to initiate, sustain and stabilize mode-locked operation. To obtain stable cw mode-locking, the spot size on the SBRs was optimized by varying the radius of curvature of the focusing mirror (150/200 mm) and by fine adjustment of the SBR position with respect to the focusing mirror. In general, a too large spot size on the SBR causes problems in initiating mode-locking or might cause q-switched mode-locked laser operation. On the other hand, a too tight focus on the SBR, might cause double pulsing (or pulse break up) and SBR damage. The necessary focusing level is also dependent on the pulsewidth and on the intracavity energy level. However, once the spot size on the SBR was adjusted to the correct range, the SBR mode-locked laser is self-starting and operates as a turn-key system for days to weeks, requiring little adjustment due to mechanical/thermal misalignments.

To demonstrate femtosecond pulses in different spectral regions, two different AlGaAs-based SBRs with central reflectivity around 800 and 850 nm were used in this study. Figure 5 shows the calculated small signal and saturated reflection curves as well as the calculated group delay dispersion curve (GDD) for the SBRs. The epitaxial growth of the SBRs were performed at the Integrated Photonic Devices and Materials Group of MIT, in a solid source, multi-wafer, dual reactor molecular beam epitaxy (MBE) system (Veeco GEN 200), at typical AlGaAs growth temperatures. The 800-nm SBR consisted of twenty five pairs of $\text{Al}_{0.95}\text{Ga}_{0.05}\text{As}$ / $\text{Al}_{0.17}\text{Ga}_{0.83}\text{As}$ quarter wave layers for the Bragg mirror stack. The low refractive index difference between $\text{Al}_{0.95}\text{Ga}_{0.05}\text{As}$ and $\text{Al}_{0.17}\text{Ga}_{0.83}\text{As}$ materials limited the reflectivity bandwidth of the SBR to 50 nm (Fig. 5). The Bragg mirror stack is followed by five pairs of 6 nm thick GaAs quantum wells to provide the saturable absorber action. The quantum wells were sandwiched between 8 nm thick $\text{Al}_{0.17}\text{Ga}_{0.83}\text{As}$ barrier layers. The last

$\text{Al}_{0.17}\text{Ga}_{0.83}\text{As}$ barrier layer had a thickness of 27 nm, which is then covered by a 5 nm thick GaAs cap layer. The thickness and the relative positions of the barrier layers and quantum wells were optimized to obtain almost wavelength independent linear and nonlinear absorption response from the absorber. Two additional pairs of $\text{SiO}_2\text{-TiO}_2$ layers were also used as a high reflection coating to reduce the modulation depth of the 800-nm SBR to $(0.6 \pm 0.2) \%$. The 800-nm SBR had a saturation energy fluence of $\sim 35 \mu\text{J}/\text{cm}^2$ and parasitic two-photon absorption (TPA) occurred for fluences above $\sim 3 \text{ mJ}/\text{cm}^2$.

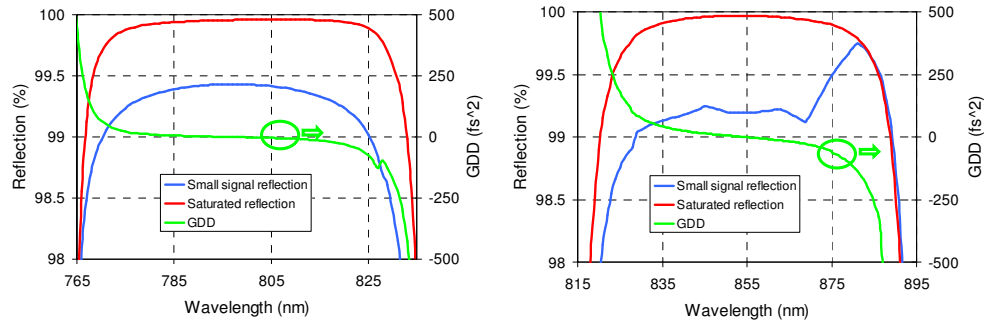


Fig. 5. Calculated small signal reflection, saturated reflection and group delay dispersion (GDD) curves for the 800 nm (left) and 850 nm (right) SBR. The calculated modulation depths were $(0.6 \pm 0.2) \%$ and $(0.8 \pm 0.2) \%$ for the 800 and 850 nm SBR, respectively.

Similarly, the 850-nm SBR consisted of twenty-five pairs of $\text{Al}_{0.95}\text{Ga}_{0.05}\text{As} / \text{Al}_{0.17}\text{Ga}_{0.83}\text{As}$ quarter-wave layers as a Bragg mirror stack and one layer of 25 nm-thick GaAs as a saturable absorber. The saturable absorber was sandwiched between 10 and 30 nm thick $\text{Al}_{0.14}\text{Ga}_{0.86}\text{As}$ barriers, and a final 5 nm thick GaAs cap layer covered the whole device. An additional $\text{SiO}_2\text{-TiO}_2$ pair was also used as a high-reflection coating on the surface. The calculated modulation depth of the 850 nm centered SBR was $(0.8 \pm 0.2) \%$.

In mode-locked laser experiments, negative cavity dispersion is also provided to operate the laser in soliton mode-locked regime [43]. In this regime, the net cavity dispersion should be adjusted to balance the self phase modulation from the crystal. The net amount of cavity dispersion together with the self phase modulation determines the output pulsewidth. Hence, one can tune the amount of cavity dispersion to adjust the pulsewidth to the desired value. We have mostly used double chirped mirrors (DCMs) for dispersion compensation in our experiments. This is because DCMs can provide almost constant group delay dispersion (GDD) in a broad wavelength range (100-150 nm), making them ideal for short pulse generation. The two kind of DCMs that were used provided -50 fs^2 and -80 fs^2 of group delay dispersions (GDD) per bounce around 800 nm. This relatively low GDD per bounce enables smooth tuning of overall cavity dispersion (hence the pulsewidth) by adjusting the number of bounces on the DCMs. However, this low GDD per bounce in general requires the usage large number of bounces on the DCMs to obtain the desired overall cavity dispersion level. Due to the above mentioned disadvantage of DCMs, in a few experiments, we have also used Gires-Tournois interferometer (GTI) mirrors, with a GDD of $\sim -550 \pm 50 \text{ fs}^2$ per bounce. The GTI mirrors had high GDD, and hence require only 1-2 bounces in order to compensate the cavity dispersion. On the other hand, their dispersion bandwidth is quite narrow, and hence they are only suitable for obtaining pulse widths around or above 100 fs.

3.2 Results of continuous-wave lasing experiments

The cw laser efficiencies of Cr:LiSAF and Cr:LiCAF at various levels of output coupling are depicted in Fig. 6. All data were taken at a base temperature of the crystal mount of 18°C . With both gain media, almost identical results were obtained using 0.5 and 1% output couplers. Due to the increased role of thermal effects, obtainable power levels decreased with 2 and 3% of output coupling. An output power as high as 500 mW was obtained at an

absorbed pump of 1145 mW with Cr:LiSAF using the 0.5% OC. The corresponding lasing threshold and the slope efficiency were 45 mW and 47%, respectively. Our estimate of the total cavity losses per round trip of approximately $(0.75 \pm 0.25) \%$ is based on measuring the lasing threshold with different output couplers (Findlay-Clay analysis [11,44]). The slope efficiency of our Cr:LiSAF laser (47%) comes close to the reported intrinsic value from the literature of 54% [31]. This fact highlights efficient mode-matching between the pump and cavity modes in our setup, which indicates the excellent beam-quality of the tapered diode laser. Moreover, the transverse mode profile of the output beam was symmetric and circular with M^2 below 1.1 in all the cases (sample measurement is shown in Fig. 7). This again is an indication of the good beam quality of the tapered diode laser. For example, Cr:Colquirite lasers pumped by multimode broad-stripe single-emitter diodes have an asymmetric and multimode laser output in the free running regime and require insertion of a slit into the cavity to operate in TEM₀₀ mode [31].

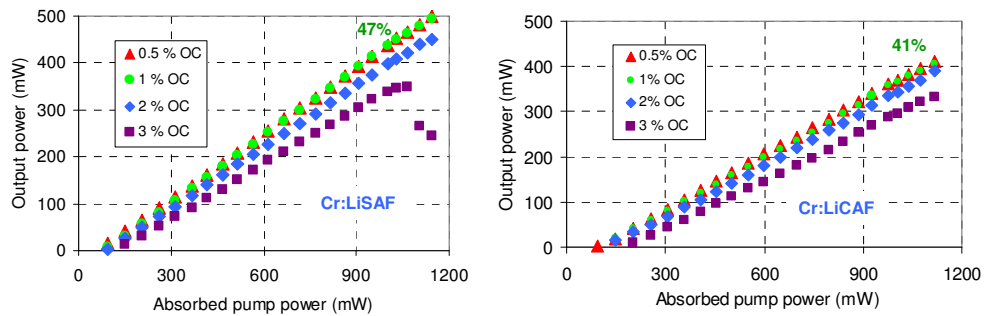


Fig. 6. Continuous-wave output power versus absorbed pump power for the single tapered diode pumped Cr:LiSAF (left) and Cr:LiCAF (right) lasers taken at various levels of output coupling between 0.5% and 3%.

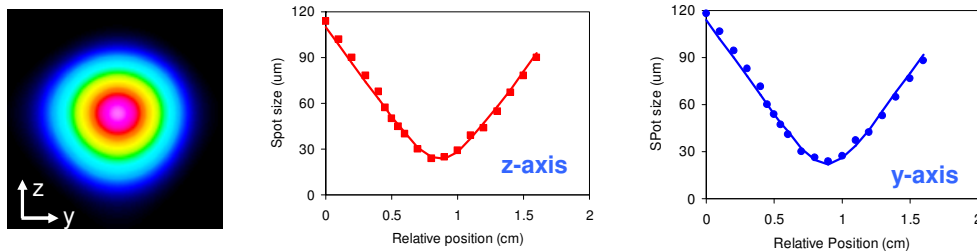


Fig. 7. (Left) Output beam profile from the Cr:LiSAF laser at the focus of a 10 cm lens. The measured spot size ($1/e^2$) distribution around the focus with the knife-edge technique in the z-axis (middle) and y axis (right). Least-squares fitting to the experimental data gave an M^2 value of 1.05 and 1.02 for the z and y axis, respectively.

An output power of 410 mW was obtained with the Cr:LiCAF laser at an absorbed pump power of 1115 mW and with a 0.5% of output coupling mirror. A lasing threshold of 93 mW and a slope efficiency of 41% have been determined for this system. As indicated by the lower output level, the total round trip losses were estimated to be approximately $(1.5 \pm 0.5) \%$ for the Cr:LiCAF cavity. A slope efficiency as high as 54% has been reported earlier from a single-mode diode pumped Cr:LiCAF laser [13]. However, that result was obtained using a higher finesse cavity with a much lower round-trip loss level (0.25%) [13]. Hence, we expect the performance to further improve in future studies with lower-loss Cr:LiCAF crystals, and lower-loss cavity optics. Especially, the Cr:LiCAF crystal that was used in this study was from a very early growth with relatively high losses ($\sim 1\%$ per cm). This high level of passive loss in Cr:LiCAF was caused mostly by micron-sized or smaller precipitates arising

during the growth process [45–47] and it is now possible to grow Cr:LiCAF crystals with passive losses below 0.2% per cm [48]. We also note that, despite the high loss Cr:LiCAF crystal that was available in this study, the slope efficiencies obtained with the tapered diode pumped system (41%), is much higher than what can be obtained (19%) while pumping with broad-stripe single-emitter diodes [31]. This is due to the good mode-matching between the tapered diode laser and the cavity mode, which cannot be attained with multimode pump sources (unless specialized cavity optics are used to obtain an asymmetric cavity mode inside the crystal that matches the asymmetric pump beam [29]).

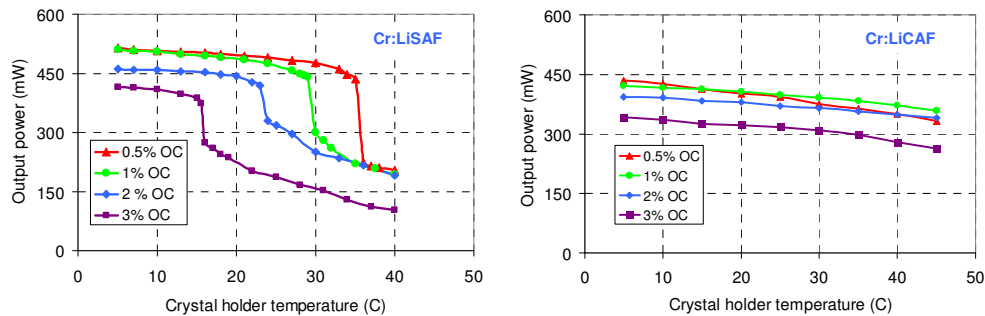


Fig. 8. Output power under cw operation at various levels of output coupling (OC) as a function of the temperature of the cooling water for the crystal holder for Cr:LiSAF (left) and Cr:LiCAF (right). The data is taken with the single TDL pumped Cr:Colquiriite laser system. The absorbed pump power was kept at a value of 1150 mW.

We have also investigated the effects of thermal loading on the laser crystals. This information was gained by measuring the cw laser performance at various temperatures of the crystal holder and with different output couplers. Figure 8 shows the measured cw laser output powers versus base temperature for the Cr:LiSAF and Cr:LiCAF lasers, at an absorbed pump power level of 1150 mW. The results show that thermal effects are less pronounced in Cr:LiCAF due to its superior thermal properties as compared to Cr:LiSAF (i.e. higher thermal conductivity, lower quantum defect due the blue shifted emission spectrum, as well as lower excited-state absorption and upconversion rate [13]). For the Cr:LiCAF laser, output power with the 0.5% output coupler increased from 410 mW to 435 mW when the crystal holder temperature was decreased from 18 °C to 5 °C. Hence; even though there is some increase in Cr:LiCAF laser output power upon cooling, our results show that the improvements are of minor importance and the tapered diode pumped Cr:LiCAF laser can be operated efficiently at room temperature.

On the other hand, a very different and interesting behavior is observed with the Cr:LiSAF laser. First of all, for each output coupling there is a critical temperature at which the laser power decreases abruptly. This finding indicates that the local temperature in some part of the Cr:LiSAF crystal reaches ~70 °C which represents a critical threshold for lifetime quenching [49]. The decrease in the upper state lifetime limits the output power by increasing the laser threshold. Secondly, the thermal effects are worse at high values of output coupling. This observation results from an Auger upconversion process in Cr:Colquiriites [31,49–51]: the lifetime of the upper laser level not only depends on temperature but also on the degree of inversion. Application of higher output coupling decreases the intracavity power which results in an increase of the population inversion of the upper laser level. In turn, the upper state lifetime decreases and laser performance degrades [31]. Note that the laser is conveniently operated at room temperature using low output coupling. For example with the 0.5% output coupler, the laser power only increases from 500 mW to 514 mW, when the crystal temperature is changed from 18 °C to 5 °C. On the other hand, our results show that the tapered diode laser pumped Cr:LiSAF system will require cooling below room temperature for applications requiring usage of higher output coupling.

3.3 Performance of mode-locked operation

In this section, representative cw mode-locking results from the tapered diode pumped Cr:LiSAF and Cr:LiCAF lasers are presented. In all cases, we kept the repetition rates around 100 MHz and the pulsewidths around 100 fs or below. Those are typical parameters desired for interesting applications like e.g. multiphoton microscopy [41].

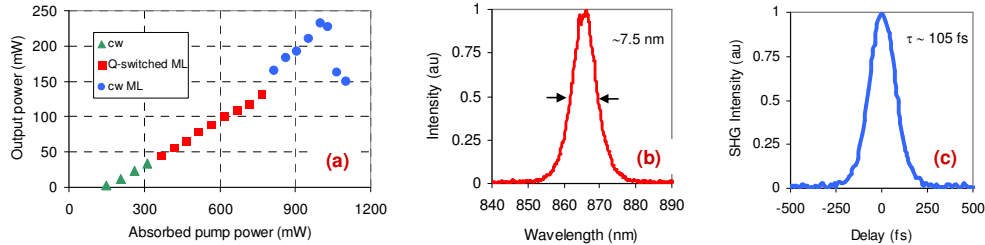


Fig. 9. Output power versus absorbed pump power (a), optical spectrum (b), and background-free intensity autocorrelation trace (c) for the 105 fs, 1.84 nJ pulses centered around 865 nm from the Cr:LiSAF laser. The laser featured a 3% output coupler and a repetition rate of 125.8 MHz.

Figure 9 summarizes representative mode-locking data of Cr:LiSAF laser around 850 nm. The 850 nm SBR was used to initiate and sustain mode-locking and DCMs were used for dispersion compensation. The estimated net cavity dispersion was about -1000 fs². Figure 9 (a) shows the variation of laser output power and laser dynamics with absorbed pump power, using the 3% output coupler. The laser operated in cw mode for absorbed pump powers up to 350 mW, and generated Q-switched mode-locked pulses for pump powers between 350 and 850 mW (Q-switched ML in Fig. 9). Stable cw mode-locking was obtained for pump powers above 850 mW (cw ML). The crystal holder was cooled to 10 °C and the maximum output power was ultimately limited by thermal effects. The laser produced 105-fs pulses (assuming sech² pulses) with 232 mW average power at an absorbed pump power of 1 W at 125.8 MHz (1.84-nJ pulse energy). The spectrum was centered near 865 nm and had a spectral bandwidth of 7.5 nm. The time bandwidth product was 0.32, close to the transform limit of 0.315 for sech² pulses.

Similarly, using a 1% output coupler, the 800 nm SBR and a GTI mirror, we have obtained a train of 90-fs pulses centered at 810 nm with an average power of 193 mW from the Cr:LiSAF laser (Fig. 10). The estimated net cavity dispersion was about -2000 fs² in this case. Interestingly, thermal effects still limited the obtainable average powers even with the 1% output coupler and at a crystal base temperature of 10 °C. We attribute this finding to the increased losses of the mode-locked laser cavity. Consequently, special low-loss DCM/GTI mirrors and SBRs will be required for optimum operation of tapered diode pumped Cr:LiSAF lasers in the mode-locked regime. This finding also suggests that tapered diode pumped femtosecond Cr:LiSAF lasers might be a good match for applications requiring the usage of low output coupling such as GHz repetition rate lasers [35], cavity-dumped lasers [52], or for lasers optimized for low timing jitter noise [53] (which requires high intracavity pulse energy and minimized cavity losses).

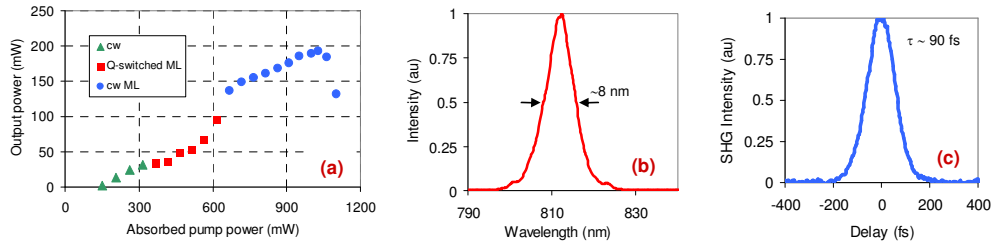


Fig. 10. Output power versus absorbed pump power (a), optical spectrum (b), background-free intensity autocorrelation trace (c) for the 90 fs, 1.97 nJ pulses centered around 810 nm from the Cr:LiSAF laser. This cavity had an output coupler of 1% and a repetition rate of 97.9 MHz.

In mode-locking experiments with the Cr:LiCAF laser, under 2% of output coupling, using DCM mirrors for dispersion compensation and the 800-nm SBR for mode-locking, we obtained pulse durations as short as 55 fs and an average output of 217 mW at an absorbed pump power of 1115 mW (Fig. 11). The estimated net cavity dispersion was about -500 fs^2 for this case. Motivated by the superior thermal properties of the Cr:LiCAF crystal, the crystal holder was cooled to only $18 \text{ }^\circ\text{C}$. Still, we did not observe a significant limitation in obtainable output powers due to thermal effects. This result shows that Cr:LiCAF is clearly the crystal of choice for power scaling experiments.

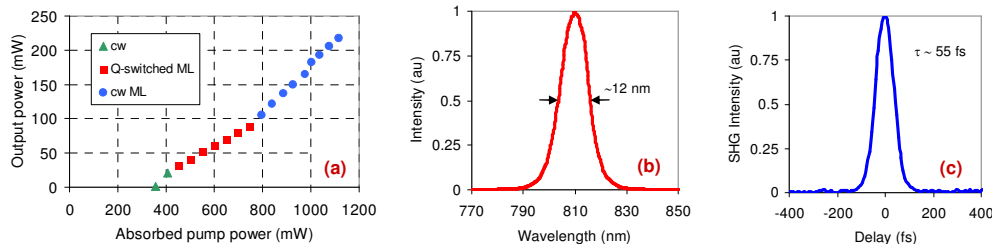


Fig. 11. Output power versus absorbed pump power (a), optical spectrum (b), background-free intensity autocorrelation trace (c) for the 55 fs, 2.04 nJ pulses centered around 810 nm from the Cr:LiCAF laser. The laser had a 2% output coupler and a repetition rate of 106.6 MHz.

4. Cr:Colquiriite Lasers Pumped by Two Tapered Diode Lasers

In this section, we will present power scalability of tapered diode pumped Cr:Colquiriite lasers upon pumping by two diodes. Our main motivation for this experiments was to build a high energy Cr:Colquiriite laser that is suitable as a pump source for femtosecond optical parametric oscillators [42].

4.1 Experimental layout of the two tapered diode laser pumped Cr:Colquiriite laser

Figure 12 shows the layout of the Cr:Colquiriite laser that is pumped by two tapered diodes (TDL-1 and TDL-2). All the parameters of the Cr:Colquiriite laser cavity were the same as described above (Section 2.2), other than the pumping geometry. As can be seen from Fig. 12, pump light from the second diode is coupled through the other side of the laser cavity. This has been done to enable a more homogeneous distribution of pump intensity inside the Cr:Colquiriite crystals which helps in limiting the thermal load on the crystals, especially due to Auger upconversion process (which scales with the square of population inversion).

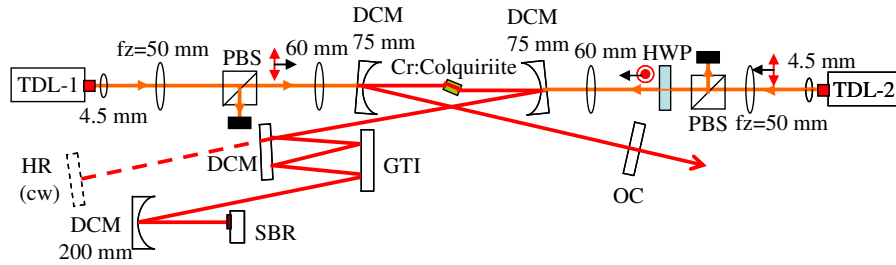


Fig. 12. Schematics of cw and mode-locked Cr:LiCAF/LiSAF oscillators pumped by two tapered diode lasers (one from each side). PBS: Polarizing beam splitter cube. HWP: Half-wave plate.

Tapered diode lasers are very sensitive to feedback, and hence we have inserted pump protection optics into the pump beam paths to prevent any feedback into the diodes from each other. This was required since 5 and 15 mW of pump light was leaking towards the other side of the pump line for Cr:LiSAF and Cr:LiCAF crystals, respectively. In order to protect the pump diodes, the polarization of the pump light from TDL-2 has been rotated 90 degrees (converted from TM to TE) using a half-wave plate (HWP). Then the transmitted light from TDL-2 was blocked by a polarizing beam splitter (PBS) cube before it reaches TDL-1 (and vice versa). The drawback of this protection scheme is the requirement to rotate the polarization of TDL-2, which results in lower efficiency with respect to incident pump power. This is because absorption of Cr:Colquiriite crystals are lower for TE polarization (95.5 for Cr:LiCAF and 91% for Cr:LiSAF), and 10% of incident light is lost due to Fresnel reflections from the crystal surface. Moreover, the PBS cubes that were used, were not optimized for our pump wavelength; hence, we had seen some additional losses from the PBS cubes. Overall we had about 940 mW of TM polarized pump light from TDL-1, and 990 mW of TE polarized pump light from TDL-2 incident on the Cr:Colquiriite crystals. We note here that, the best solution to all of these problems is to use Cr:Colquiriite crystals with even higher absorption (slightly longer crystals and/or slightly higher doped crystals), which might enable 10-20% better results than those reported below.

4.2 Results of continuous-wave lasing experiments

The cw laser efficiencies of Cr:LiSAF and Cr:LiCAF that was observed with the two TDL pumped system at various levels of output coupling are depicted in Fig. 13. Similar to the single tapered diode pumped system, all data were taken at a base temperature of the crystal mount of 18 °C. The dashed line marks the point where we started to use the pump light from TDL-2. With Cr:LiSAF gain media, using a 0.5% output coupler, we have obtained output powers as high as 850 mW at an absorbed pump power level of 1740 mW (total incident power was 1930 mW). The corresponding slope efficiency with respect to the absorbed pump power was 49%, which is slightly higher than what we obtained (47%) from the single TDL pumped system. This we believe might be due to a slight improvement in cavity alignment, and/or slight improvement in thermal effects due to the increased intracavity power levels. The efficiency curve for Cr:LiSAF laser with the 3% output coupler shows a more interesting behavior. When only TDL-1 is used, we see a roll off in output powers at high incident pump powers due to thermal effects. However, when we also pump with TDL-2, we start to see an increase in output power due to an improvement in thermal effects. This is because TDL-2 pumps the right side of the crystal, so it does not create any significant additional thermal load on the left side. Moreover, due to an increase in circulating intracavity laser power, the laser inversion level is lower. This lowers the rate of Auger upconversion and hence decreases the thermal load on the crystal, which results in improved thermal performance.

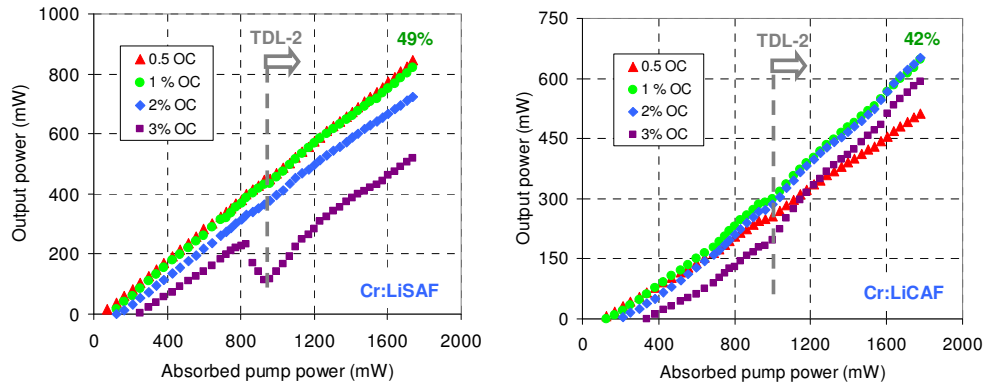


Fig. 13. Continuous-wave output versus absorbed pump power for the Cr:LiSAF (left) and Cr:LiCAF (right) lasers pumped by two TDLs, taken at various levels of output coupling between 0.5% and 3%.

An output of 650 mW was obtained with the Cr:LiCAF laser at an absorbed pump power of 1780 mW with a 1% output coupler. The corresponding slope efficiency was 42%. Similar to the Cr:LiSAF, we see a noticeable increase in laser performance with the 3% output coupler. However, the effect is not as significant as Cr:LiSAF due to the better thermal performance of Cr:LiCAF gain medium.

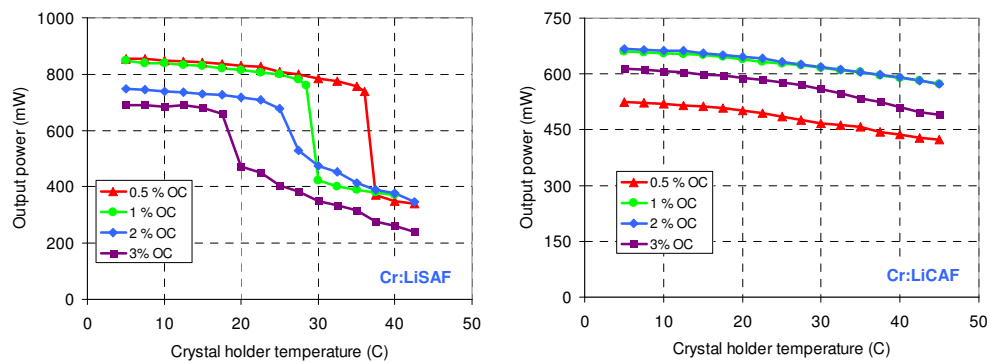


Fig. 14. Output power under cw operation at various levels of output coupling (OC) as a function of the temperature of the cooling water for the crystal holder for Cr:LiSAF (left) and Cr:LiCAF (right). The data is taken with the two TDL pumped Cr:Colquiriite laser system (one from each side), and the absorbed pump power was kept at a value of about 1800 mW.

We have also investigated the variation of laser output power with crystal holder temperature for the double TDL pumped system (Fig. 14). For Cr:LiCAF, the measured variation of output power with crystal holder temperature is very similar to what we have measured earlier with the single TDL pumped system (Fig. 8). We basically observe a slow decrease in output power with increasing temperature; and the data shows that the Cr:LiCAF laser could be operated at room temperature without any significant thermal problem. Similarly, with Cr:LiSAF gain media the observed trend is familiar. However, compared to the single TDL pumped system, there is a slight increase in the critical temperature where we observe the sharp decrease in output power. For example, for the 3% output coupler, the critical crystal holder temperature where we observe the sharp decrease in power increased from about 16 °C to 20 °C. As mentioned above, we believe that this improvement is due to the decreased role of Auger upconversion rate upon increase in intracavity power levels.

4.3 Mode-locked Cr:LiCAF laser with high pulse energy for OPO applications

Femtosecond optical parametric oscillators (OPOs) synchronously pumped by Ti:Sapphire lasers enable the generation of tunable femtosecond pulses in the near and mid-infrared spectral region (1000-4000 nm). The second harmonic of these pulses further enable the extension of this tuning range into the visible (500-750 nm), which is hard to access otherwise. However, cost and complexity of Ti:Sapphire lasers are also an issue limiting the widespread usage of the OPO technology. Ideally, Cr:Colquiriite laser pumped OPOs can enable the reduction of cost, and might promote the extensive usage of this technology. However, to our knowledge, Cr:Colquiriite laser pumped femtosecond OPOs have not been demonstrated yet. This is mainly due to the low pulse energies available from Cr:Colquiriite lasers, which is barely enough to reach the lasing threshold of optical parametric oscillators [42].

With the recent progress in laser diode technology during the last 5 years or so, pulse energies from standard 100 MHz Cr:Colquiriite lasers recently became reasonable enough for OPO pumping applications (~2 nJ). In the mode-locking experiments with the double side-pumped system, we aimed to build a high energy Cr:Colquiriite laser optimized for synchronous OPO pumping. We have chosen to work with the Cr:LiCAF crystal, as it proved itself more suitable and easier to work with at high powers. With respect to the pulsewidth of the Cr:LiCAF laser, we chose to operate the laser with relatively long pulses (200-300 fs level) due to the fairly large group velocity mismatch in typical nonlinear OPO crystals. For example, for PPMgO:LN crystal (MgO-doped LiNbO₃), the group velocity mismatch between a 810 nm pump pulse and 1250 nm signal pulse is about 225 fs/mm [54]. Hence, for typical crystal length of 1 mm, the optimum pulsewidth is about 225 fs.

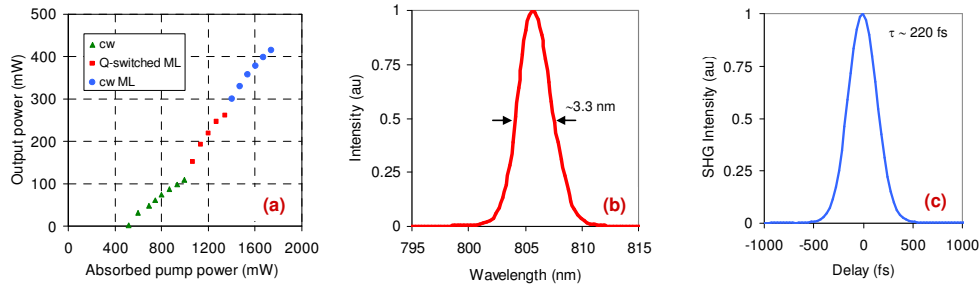


Fig. 15. Output power versus absorbed pump power (a), optical spectrum (b), background-free intensity autocorrelation trace (c) for the 220 fs, 5.4 nJ pulses centered around 807 nm from the Cr:LiCAF laser. The laser had a 3% output coupler and a repetition rate of 77 MHz.

Motivated by the arguments above, we have obtained the mode-locking results summarized in Fig. 15 from the double TDL pumped Cr:LiCAF laser. The higher pulse energies and the long pulsewidths required relatively large amount of net negative dispersion. Hence, the results in Fig. 15 have been taken from a cavity, in which we had four bounces on the GTI mirror in a round-trip (Fig. 12). This enabled a net cavity dispersion level of about -2500 fs². The Cr:LiCAF crystal holder was cooled to only 18 °C. Using the 3% output coupler and the 800-nm SBR for mode-locking, the Cr:LiCAF laser produced 220 fs long pulses with an average output of 415 mW at an absorbed pump power of 1740 mW. This corresponds to a pulse energy of 5.4 nJ at the repetition rate of 77 MHz. To our knowledge, these are the highest pulse energies that are obtained from any standard configuration femtosecond Cr:Colquiriite laser to date. Earlier studies have shown that reaching higher pulse energies require non-standard techniques such as using lower-repetition rate cavities (~10-nJ at 10 MHz [55]), or using the cavity-dumping concept (~100-nJ at 50 kHz [52]), which are not suitable for synchronous OPO pumping experiments.

5. Summary and Future Work

In summary, we have presented cw and cw mode-locked operation of Cr:LiSAF and Cr:LiCAF lasers that are pumped by a tapered diode laser. Our results show that a single pump device is sufficient to reach attractive levels of output power from Cr:Colquiriites. We have also shown that pumping with two diodes enables average power scaling to record levels for Cr:Colquiriite systems. Moreover, compared to systems that are pumped by four single or multimode diodes, the tapered diode pumped system is compact, less complex, more efficient and therefore features reduced alignment sensitivity and enhanced long-term stability. Therefore, we are convinced that such low-cost and high-brightness tapered diodes in the red spectral region will become the standard pump source for Cr:Colquiriite lasers in the near future.

During the experiments, we have observed some thermal effects in Cr:LiSAF, but there is great potential to reduce them in future studies by using thinner gain crystals with optimized Cr-doping and by using optimized intracavity optics with lower loss. As an alternative, usage of Cr:LiSGaF crystal might also help with thermal effects. Cr:LiSGaF has almost identical spectroscopic parameters as Cr:LiSAF [13], but has slightly increased thermal performance, and should enable improved power scaling than Cr:LiSAF in the 850 nm region. However, we should note that, among Cr:Colquiriites, with its superior thermal properties, Cr:LiCAF should be the crystal of choice for applications requiring higher average powers. This is already demonstrated in part by the two tapered diode pumped Cr:Colquiriite laser experiments that we have performed in this study.

We also note here that, there is great potential in future improvement of mode-locked laser performance of tapered diode pumped Cr:Colquiriite systems. In particular, the representative mode-locking results that we chose to present in this study showed pulsewidths in the 50-250 fs range. However, earlier studies have shown that, with fine dispersion adjustment with prism pairs, it is possible to obtain pulsewidths of ~25-fs from standard AlGaAs-based SBR mode-locked Cr:Colquiriite lasers [34]. Also, using novel oxidized broadband SBR mirrors [56], it might be possible to obtain down to ~10-fs level pulses from Cr:Colquiriites. Moreover, despite their low nonlinear coefficient, stable Kerr-lens mode-locked operation might also be feasible in Cr:Colquiriites using gain matched output couplers [57], which could also enable ultra short (~10-fs) pulse generation [15,17]. In terms of tuning in femtosecond regime, we have only presented mode-locking at fixed wavelengths around 800 nm and 850 nm in this study. However, as earlier studies have shown, it is possible to obtain tunable femtosecond mode-locked operation in Cr:Colquiriites. Using standard AlGaAs-based SBRs around 800, 850 and 900 nm, fs tuning ranges of 767-817 nm with Cr:LiCAF, and 803-831 nm (28 nm), 828-873 nm (45 nm) and 890-923 nm (33 nm) with Cr:LiSAF have been demonstrated [34]. Similarly, usage of oxidized broadband SBRs should also enable tunable sub-100-fs pulses from ~750 nm to ~1000 nm from Cr:Colquiriites [56].

Pulse energies and peak powers that were obtained in this study were in the 5 nJ and 50 kW range, respectively. This pulse energy and peak power levels are suitable for many application, but some other applications like femtosecond micromachining [58] or deep multiphoton microscopy imaging [59,60] might require higher pulse energies and/or peak powers. We believe that the peak powers can be scaled up to ~100-200 kW level by building multi-pass cavity Cr:Colquiriite lasers at ~10 MHz repetition rate [55], or to the ~1-2 MW level by cavity-dumped Cr:Colquiriite lasers with pulse repetition rates up to 50-kHz [52]. Moreover, improvements in output power of tapered diode lasers are expected to enable further average and peak power scaling.

In short, we have shown that the recent advances in tapered diode technology enabled the construction of compact, efficient, and high-power Cr:Colquiriite laser systems. We believe that, with the ongoing improvements, femtosecond Cr:Colquiriite lasers have the potential to become a versatile, low-cost femtosecond source for several important application areas in science and engineering.

Acknowledgments

We thank Christian Beschle, Günther Krauss, Daniele Brida, Stefan Eggert, Sören Kumkar and Marcel Wunram from Konstanz University, Alphan Sennaroglu from Koç University, and Duo Li, Jing Wang, Sheila Nabanja, Peter Fendel, and Jonathan Birge from Massachusetts Institute of Technology for their help. We also thank the anonymous reviewer for his/her constructive suggestions. We acknowledge partial support from the Center for Applied Photonics of Konstanz University, and by AFOSR contracts FA9550-10-1-0063 and FA9550-07-1-0101, NSF ECCS-0900901 and Thorlabs Inc. Umit Demirbas acknowledges postdoctoral fellowship support from Alexander von Humboldt-Foundation.